Original Article

Optimization of determinant factors associated with the efficiency of experimental autoimmune uveitis induction in C57BL/6 mice

Ming Yang[1#], Zixuan Yang[1#], Jiani Huang[1], Wangshu Yu[2], Xiaoying He[1], Minjie Yuan[1], Wei Han[1^], Wei Chen[3^]

[1]Eye Center of the Second Affiliated Hospital, School of Medicine, Zhejiang University, Hangzhou, China; [2]Department of Ophthalmology, The First Affiliated Hospital, School of Medicine, Zhejiang University, Hangzhou, China; [3]Institute of Immunology, School of Medicine, Zhejiang University, Hangzhou, China

Contributions: (I) Conception and design: W Chen, W Han; (II) Administrative support: M Yang, Z Yang, J Huang, W Yu, X He, M Yuan, W Han, W Chen; (III) Provision of study materials or patients: M Yang, Z Yang, X He, M Yuan, W Han, W Chen; (IV) Collection and assembly of data: M Yang, Z Yang, J Huang, W Yu; (V) Data analysis and interpretation: M Yang, Z Yang; (VI) Manuscript writing: All authors; (VII) Final approval of manuscript: All authors.

[#]These authors contributed equally to this work and should be regarded as co-first authors.

Correspondence to: Wei Chen. Institute of Immunology, School of Medicine, Zhejiang University, 866 Yuhangtang Road, Hangzhou 310058, China. Email: chenwei566@zju.edu.cn; Wei Han. Eye Center of the Second Affiliated Hospital, School of Medicine, Zhejiang University, 88 Jiefang Road, Hangzhou 310003, China. Email: hanweidr@zju.edu.cn.

Background: Experimental autoimmune uveitis (EAU) is a widely used animal model for uveitis research. The C57BL/6 mouse strain is the most commonly used mouse strain in the research of genetic modification, but C57BL/6 mice are not sufficiently susceptible to EAU induction, partly due to experimental factors. This work aims to optimize relevant factors to improve the efficiency of EAU induction in C57BL/6 mice.

Methods: To induce EAU, mice were immunized via intraperitoneal injection with pertussis (PTX) and subcutaneous injection with interphotoreceptor retinoid-binding protein peptide 1–20 ($IRBP_{1-20}$) emulsified with complete Freund's adjuvant (CFA). The severity of inflammation was assessed using several approaches. The relevant experimental factors were evaluated, including methods of emulsification and doses of peptide and PTX.

Results: Uveitis occurred at 8–12 days after immunization and reached its peak at 18–20 days, while T helper type 17 (Th17) cells peaked earlier at 14–18 days after immunization. Based on clinical and histological scores, 500 μg of IRBP peptide was the optimal dose required to induce EAU. The PTX dose demonstrated no influence on EAU incidence, but potentially affected the severity of uveitis. A single injection of 1,000 ng of PTX induced the most severe EAU and the highest proportion of Th17 cells. Compared to extruded emulsion, sonicated emulsion produced a higher incidence, higher histological score, and a 2-day-earlier onset of EAU. Electron microscopy showed a significantly different microstructure between the 2 emulsions.

Conclusions: This work optimized the protocols of EAU induction and obtained a high and stable induction rate with severe inflammation in the C57BL/6 mouse strain. Our results facilitate future experimental research involving uveitis.

Keywords: Experimental autoimmune uveitis (EAU); C57BL/6 mice; pertussis; autoimmunity; induction protocol

Submitted May 01, 2022. Accepted for publication Sep 19, 2022.
doi: 10.21037/atm-22-2293
View this article at: https://dx.doi.org/10.21037/atm-22-2293

^ ORCID: Wei Han, 0000-0003-1696-0615; Wei Chen, 0000-0002-2339-5741.

Introduction

Uveitis is one of the most common ocular diseases causing blindness (1). Based on causes of the disease, uveitis can be categorized into 2 types: infectious uveitis and noninfectious uveitis. Infectious uveitis is usually caused by viruses, bacteria, parasites, and other infectious reasons, while noninfectious uveitis is generally associated with autoimmunity (2,3). However, the specific etiology of uveitis is far from being fully elucidated. Understanding the exact etiology is of great importance for the treatment of uveitis and the prevention of vision loss.

Experimental autoimmune uveitis (EAU) induced in mice is the most widely adopted rodent model in the research of autoimmune uveitis by active immunization with human interphotoreceptor retinoid-binding protein (IRBP) (4). The susceptibility and the severity of EAU can vary among different mice strains (5), among which B10.BIII and C57BL/6 are the most commonly used. These 2 strains differ greatly with respect to EAU reactions. B10.RIII is the most susceptible strain for EAU. After immunization, B10.BIII mice exhibit a quick and severe inflammatory response, which can be potentially complicated with retinal detachment and subretinal hemorrhage (6). Despite the merit of consistent and robust inflammatory reaction, the weakness of EAU established in B10.BIII mice strain is also obvious. The rapid destruction of the retina and permanent loss of visual function in B10.BIII mice are not consistent with the natural course of human uveitis, which usually develops slowly and has a prolonged course (7). In contrast, immunized C57BL/6 mice develop chronic inflammation with recurring and persistent retinitis combined with mild to moderate destruction of visual function (8). Moreover, the inflammation mainly involves the posterior segment of the eyes, which is the most common form of human sight-threatening uveitis. Importantly, the C57BL/6 mouse strain offers the most complete, commercially available model of transgene and gene knockout, allowing multiple approaches to the in-depth study of EAU. Thus, the C57BL/6 mouse strain is currently thought to be an ideal mouse strain for uveitis research.

Nevertheless, a dilemma still exists. The unstable incidence of EAU and the low to moderate levels of inflammation limit the broad application of C57BL/6 mice (9). Compared with B10.BIII mice, C57BL/6 mice have only moderate susceptibility to EAU induction and require additional intraperitoneal injections of pertussis (PTX) while being subcutaneously immunized (10). Owing to the unstable susceptibility, the incidence of EAU, the severity of inflammation, and the peak of uveitis are highly variable across different studies using the C57BL/6 mouse strain, leading to indeterminacy for induction (11-14). Multiple factors, especially emulsification and the dose of $IRBP_{1-20}$ peptide and PTX, can influence the incidence of EAU (9). Therefore, optimizing relevant factors to obtain a stable and high induction rate of EAU is essential for uveitis research. This work investigated the effects of several major determinants on the induction of EAU in C57BL/6 mice, including a dose of peptide, dose and usage of PTX, and methods of emulsification. The progress of EAU inflammation was evaluated via ophthalmoscopy, hematoxylin and eosin (HE) staining, retinal whole flat mounts, and lymphocyte flow analysis. The conditions of peptide, PTX, and emulsion were optimized to obtain the stable and sufficient induction of EAU in the C57BL/6 strain. We present the following article in accordance with the ARRIVE reporting checklist (available at https://atm.amegroups.com/article/view/10.21037/atm-22-2293/rc).

Methods

Animals

Female C57BL/6J mice (stock No. 000664), aged 6–8 weeks, were purchased from Shanghai Model Organisms Center Inc. (Shanghai, China). Mice were kept in accordance with the Association for Research in Vision and Ophthalmology (ARVO) statement for the Use of Animals in Ophthalmic and Vision Research. All mice were housed in high-level sterilization, specific pathogen-free (SPF) facilities and were randomly assigned a group. All animal experiments were approved by an animal experimental ethical inspection of the First Affiliated Hospital, College of Medicine, Zhejiang University (Ethical Approval No. 2019-23-1) and were carried out in accordance with the Guide for the Care and Use of Laboratory Animals, 8th edition. The animal numbers and the results obtained via different assessment approaches are summarized in *Table 1*. The number of mice is normally around 10 per group in an *in vivo* study. We prepared more than 10 mice for each group to allow for accidental death. Based on the high quality of antigen-adjuvant emulsion, enough samples for each group were obtained if at least 10 mice were successfully immunized and survived until the day for sacrifice.

Table 1 Overview of animal numbers and results obtained via different approaches

Induction protocol	Total number of mice	Number of EAU mice	Mean clinical scores (mean ± SEM)	Mean histological scores (mean ± SEM)	$CD4^+$ $IL\text{-}17A^+$% (n=5) (mean ± SEM)
$IRBP_{1\text{-}20}$: 200 µg; PTX: 500 ng; extruded emulsion; days post immunization as indicated					
Day 7	15	1	0.00±0.00	0.03±0.03	1.12±0.10
Day 10	10	2	0.05±0.05	0.10±0.07	1.19±0.26
Day 14	10	3	0.20±0.11	0.20±0.11	3.50±0.34
Day 18	12	5	0.55±0.26	0.38±0.18	3.85±0.34
Day 22	11	4	0.40±0.22	0.27±0.12	2.99±0.16
Day 26	11	3	0.25±0.13	0.18±0.10	1.65±0.32
$IRBP_{1\text{-}20}$: as indicated; PTX: 500 ng; extruded emulsion; 18 days postimmunization					
200 µg	17	7	0.60±0.26	0.29±0.10	3.99±0.33
500 µg	19	8	0.90±0.34	0.55±0.14	4.45±0.31
700 µg	16	3	0.35±0.21	0.13±0.07	3.91±0.43
$IRBP_{1\text{-}20}$: 500 µg; PTX: as indicated; extruded emulsion; 18 days postimmunization					
300 ng	17	7	0.35±0.15	0.24±0.08	1.84±0.13
500 ng	18	8	0.75±0.29	0.56±0.18	4.49±0.57
1,000 ng	19	10	1.10±0.38	1.08±0.28	5.26±0.16
1,500 ng	17	7	0.65±0.26	0.50±0.17	2.96±0.07
2,500 ng	16	7	0.80±0.29	0.81±0.28	4.72±0.65
$IRBP_{1\text{-}20}$: 500 µg; PTX: 1,000 ng; 18 days postimmunization					
Extruded emulsion	18	9	1.60±0.45	1.06±0.29	5.31±0.55
Sonicated emulsion	17	14	2.20±0.44	1.97±0.34	7.53±0.36
$IRBP_{1\text{-}20}$: 500 µg; PTX: 1,000 ng; sonicated emulsion; days postimmunization: as indicated					
Day 7	12	2	0.20±0.11	0.08±0.06	1.39±0.18
Day 14	12	8	2.00±0.37	0.88±0.23	3.58±0.86
Day 18	17	14	2.20±0.44	1.97±0.34	7.53±0.36
Day 22	11	8	1.60±0.31	1.80±0.42	6.08±0.56

EAU, experimental autoimmune uveitis; IRBP, interphotoreceptor retinoid-binding protein; PTX, pertussis; SEM, standard error of the mean; IL-17, interleukin 17.

EAU induction and preparation of the antigen-adjuvant emulsion

To induce EAU, different doses of $IRBP_{1\text{-}20}$ peptide (GPTHLFQPSLVLDMAKVLLD) suspended in 100 µL of phosphate-buffered saline (PBS) were emulsified with an equal volume of complete Freund's adjuvant (CFA; Sigma-Aldrich, St. Louis, MO, USA) containing 2.5 mg/mL of *Mycobacterium tuberculosis* strain H37RA (Sigma-Aldrich). Mice were immunized with a subcutaneous injection of 200 µL of emulsion mixture and an intraperitoneal (i.p.) injection of 100 µL of PTX toxin of different concentrations. A protocol was prepared before the study without registration. The mice were killed humanely by cervical dislocation at different time points after immunization.

To prepare the antigen-adjuvant emulsion, extrusion was performed with 2 syringes connected by a 3-way cock, and the quality of emulsion was taken as good if the

emulsion did not spread and remained as droplets on the water surface for 2 hours. Sonication was performed in a round-bottomed plastic tube with a probe immersed under the liquid level and at 50% amplitude (VXC130, Sonics & Materials, Newtown, CT, USA) adopted for 5 min with a pulse of 5 s/6 s (on/off). The quality of sonicated emulsion was also evaluated on the water surface in similar fashion to that of the extruded emulsion.

Assessment of EAU by fundoscopy and histology

Under anesthetization by pentobarbital sodium (i.p.), clinical scoring of ocular inflammation was constructed by fundoscopy on a scale of 0 to 4, as described previously (8,15). The 2 eyes of each mouse were evaluated, and the average score of the 2 eyes was used.

For histology, eyes were harvested at different time points after immunization, fixed in ophthalmic fixation solution [80% isopropanol, 25% acetic acid, and 37% formaldehyde (8:1:1; v/v/v)] overnight, and embedded in paraffin. Eyes were sectioned through the pupillary-optic nerve axis and stained with HE. All the histological samples were processed by 1 person following the same staining protocol. Experienced investigators (blinded to the immunization groups) evaluated the severity of EAU on a scale of 0 to 4 according to the published criteria including the number, type, and size of lesions (15,16). Two independent investigators completed the assessment based on the low and high magnification images. Scores that were obviously different between the 2 independent investigators were arbitrated by a third experienced investigator.

Flow cytometry

The single-cell suspension was isolated from the draining lymph node (dLN) by the traditional method. Cells were cultured with 200 ng/mL of phorbol 12-myristate 13-acetate (PMA; Merck, Darmstadt, Germany) and 500 ng/mL of ionomycin (Merck) for 4 hours, which was followed by the addition of brefeldin A (BFA; 1 μg/mL; Sigma-Aldrich) 0.5 h later. After being rinsed, cells were resuspended with 50 μL of PBS, and extracellular staining was performed with 0.3 μL of CD4-fluorescein isothiocyanate (FITC; BD Bioscience, San Jose, CA, USA). Cells were then fixed and permeabilized with the intracellular fixation buffer (Fix/Perm Cell Permeabilization Kit; eBioscience, San Diego, CA, USA) for 20 min, which was followed by intracellular staining with interleukin 17 A (IL-17A) for 30 min. The relevant isotype mAb (eBioscience) was used as the fluorescence minus one (FMO) control. The positive cells were detected by the ACEA Novocyte flow cytometry (ACEA Biosciences, San Diego, CA, USA), and data were processed with the FlowJo software v. 10.4.0 (FlowJo LLC, Ashland, OR, USA)

Electron microscopy

To visualize the emulsion by transmission electron microscopy (TEM), the samples were dispersed in double-distilled water (ddH_2O) and processed by negative staining. To this end, 10 μL of emulsion was pipetted onto carbon film and preliminarily hydrophilized by a glow discharge instrument and then incubated for 1 min. The carbon film was washed twice by ddH_2O and stained with 5 μL of 2% uranium acetate for 1 min. The staining solution was discarded, and the carbon film was dried. The images were acquired with a 120 kV transmission electron microscope (Tecnai G2 Spirit; FEI Co., Hillsboro, OR, USA) (17).

Immunofluorescence

The isolated eyeballs were fixed in 4% paraformaldehyde for 1 h, and the retinal whole mounts were prepared. After being treated with the blocking buffer [15% normal goat serum plus 1% Triton X-100 (Sigma-Aldrich) in PBS] for 4 h at room temperature, the mount was incubated with rabbit anti–CD4 antibody (1:100; Abcam, Cambridge, UK) and FITC-conjugated isolectin B4 (1:100; Sigma-Aldrich) overnight at 4 ℃. After a wash with PBS 3 times, Alexa Fluor 555 goat anti-rabbit (1:1,000; Invitrogen Inc., Thermo Fisher Scientific, Waltham, MA, USA) was used as the secondary antibody. The stained retina was then flattened and mounted onto a glass slide and covered by a coverslip with fluorescent mounting medium using 4, 6-diamidino-2-phenylindole (DAPI; ZLI-9557, ZSGB-Bio, Beijing, China).

Statistical analysis

The data were processed with GraphPad Prism software (GraphPad Software Inc., La Jolla, CA, USA) and are presented as mean ± standard error of the mean (SEM). Histopathological results were analyzed by the Mann-Whitney or Kruskal-Wallis test. The flow cytometry data were analyzed by the Student's *t*-test or one-way analysis of variance (ANOVA). A P value of <0.05 was considered statistically significant.

Table 2 Immunization protocols in different studies

Researcher	Dosage of $IRBP_{1-20}$ (μg)	Dosage of PTX (ng)	Incidence	Histological scoring
Yadav *et al.* (12)	100	500	Not mentioned	3.12
Avichezer *et al.* (18)	150	1,500	86%	0.7
Fukushima *et al.* (19)	150	1,500	40%	0.29
Fang *et al.* (11)	150	500	Not mentioned	~0.7
Santeford *et al.* (20)	200	300	Not mentioned	~0.4
Ke *et al.* (21) (an adoptive transfer model of EAU)	200	500	Not mentioned	Not mentioned
Hsu *et al.* (22)	200	1,500	78%	2.3
Cortes *et al.* (23)	300	400	40%	0.5
Mattapallil *et al.* (10)	300	500	82%	~0.4
Pan *et al.* (24)	350	1,000	Not mentioned	~0.7
Huang *et al.* (25)	500	1,000	Not mentioned	~1.7

IRBP, interphotoreceptor retinoid-binding protein; PTX, pertussis; EAU, experimental autoimmune uveitis.

Results

Indicators and relevant time windows for the evaluation of inflammation in EAU

According to the previous literature (*Table 2*), the protocol of commonly used dosages (200 μg $IRBP_{1-20}$ and 500 ng PTX) was adopted. The eye fundus score was recorded via fundoscopy throughout the induction process. The eyeballs and dLNs were collected at different time points. The EAU inflammation was assessed by histology section, retinal flat mounts, and flow cytometry.

Fundoscopy showed that the onset of clinical symptoms started 8 to 12 days after immunization, and inflammation was aggravated continuously and reached a peak level at days 18 to 20 after immunization and was followed by the fading of inflammation (*Figure 1A*). Consistent with the clinical score, the HE score reached a peak level at day 18 (*Figure 1B,1C*). Our data were in line with previous reports in the literature on the EAU peak on days 16–21 (26,27). For retina flat mounts, FITC-conjugated isolectin-B4 (IB4) was adopted to identify both blood vessels and leukocytes, and $CD4^+$ cells were identified by the specific immunofluorescent staining. The retinal flat mounts revealed that a large number of $CD4^+$ T cells infiltrated the large blood vessels in the optic disc zone, which coincided with the progression pattern of pathological scores (*Figure 1D*). The flow cytometry showed that the proportion of T helper type 17 (Th17) cells reached a high level at 14–18 days and decreased at day 22 (*Figure 1E,1F*).

Overall, our data revealed that EAU inflammation peaked at around day 18 and then dissipated. Day 18 might be the optimal time point to assess EAU inflammation. The peaks of inflammatory cell infiltration and pathological scores in the retinal tissue were highly consistent. The expansion of Th17 cells in the dLN occurred prior to the relevant inflammatory manifestations in the retina.

The optimal dosage of $IRBP_{1-20}$

To explore the effect of $IRBP_{1-20}$ dosages on EAU induction, 3 different doses (low: 200 μg; moderate: 500 μg; high: 700 μg) were used. C57BL/6 mice were immunized using a subcutaneous injection with peptide emulsion and an intraperitoneal injection with 500 ng of PTX simultaneously. The mice were sacrificed 18 days after immunization.

The clinical scores evaluated by fundoscopy showed that the severity of inflammation in the moderate-dose group (500 μg) was higher than that in the low-dose (200 μg) and high-dose groups (700 μg; *Figure 2A*). According to the histological results, the incidence of EAU in the low-dose (200 μg) and moderate-dose group (500 μg) was around 40%, while the incidence in the high-dose group (700 μg) was lower (approximately 19%; *Figure 2B*). Histological scoring showed more severe inflammatory damage in the moderate-dose group (score approximately 0.5) than in the low-dose (score approximately 0.3) and high-dose groups (score approximately 0.1; $P<0.05$; *Figure 2C,2D*). For the retina flat mounts, the most obvious infiltration of $CD4^+$ T cells was observed in the moderate-dose group (500 μg; *Figure 2E*). The proportion of Th17 cells in the

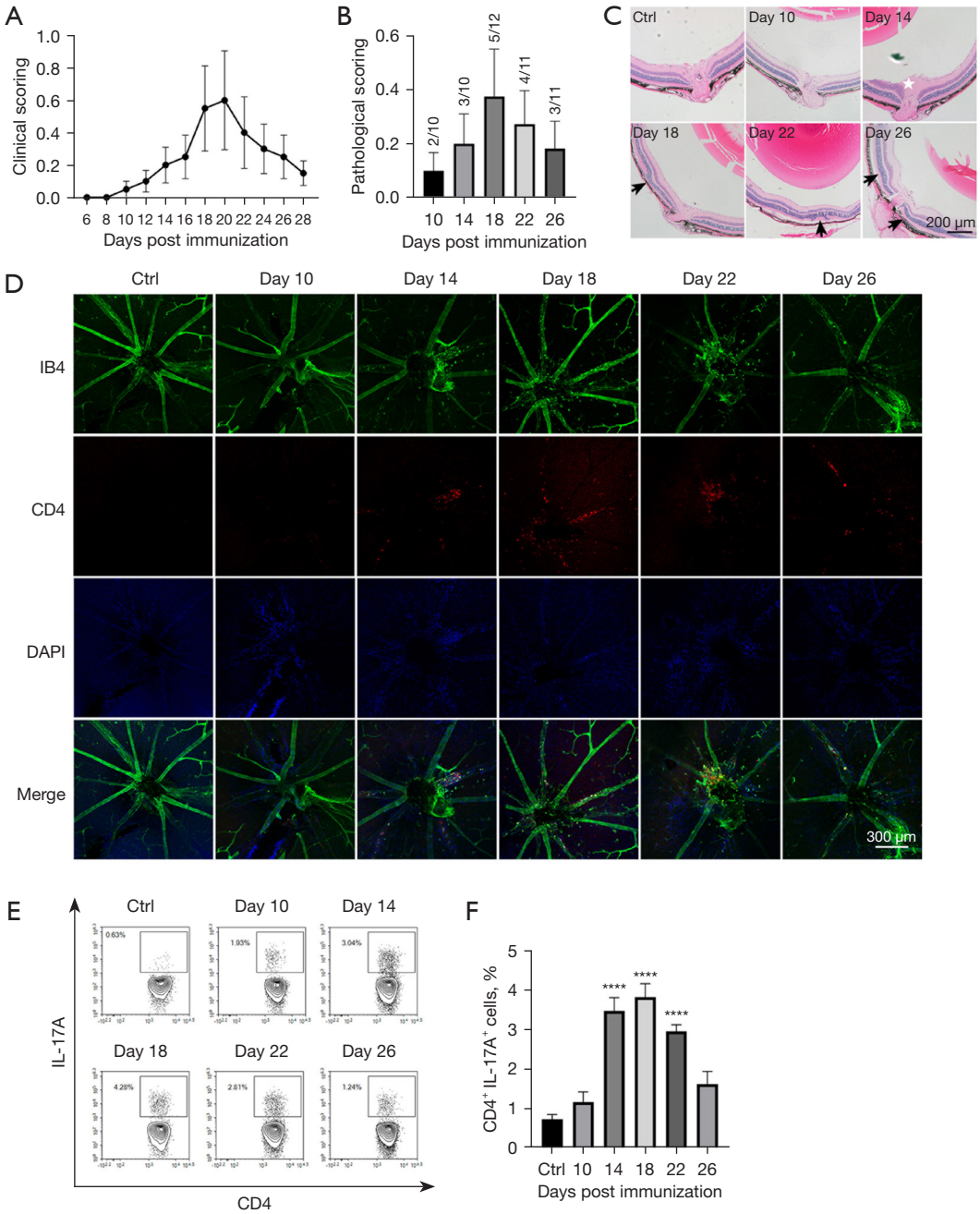

Figure 1 Different observational indices used to estimate inflammation in EAU. EAU was induced in C57BL/6 mice (female, 6–8 weeks) by immunization with 200 μg of $IRBP_{1-20}$ emulsified in CFA, with an intraperitoneal injection of 500 ng PTX simultaneously. (A) Clinical scores at indicated time points postimmunization (n≥10). (B) Mean pathological scores of HE retinal sections. The overall pathological scores include mice with EAU and mice without EAU (score 0). The number (for example "2/10") represents EAU mice/total immunized mice. (C) Representative HE staining of the retinal section at different time points (black arrow: retinal folds; white star: edema; scale bar: 200 μm). (D) Representative immunofluorescent staining images for retina flat mounts (IB4: green; $CD4^+$ cells: red, DAPI: blue; scale bar: 300 μm). (E,F) Representative images of flow cytometry and ratios of $CD4^+IL\text{-}17A^+$ cells in dLN, gated on $CD4^+$ cells (n=5); ****, P<0.0001 compared to control. All data are presented as mean ± SEM. EAU, experimental autoimmune uveitis; IRBP, interphotoreceptor retinoid-binding protein; CFA, complete Freund's adjuvant; PTX, pertussis; HE staining, hematoxylin and eosin staining; IB4, isolectin-B4; DAPI, 4,6-diamidino-2-phenylindole; IL-17, interleukin 17; dLN, draining lymph node; ctrl, control; SEM, standard error of the mean.

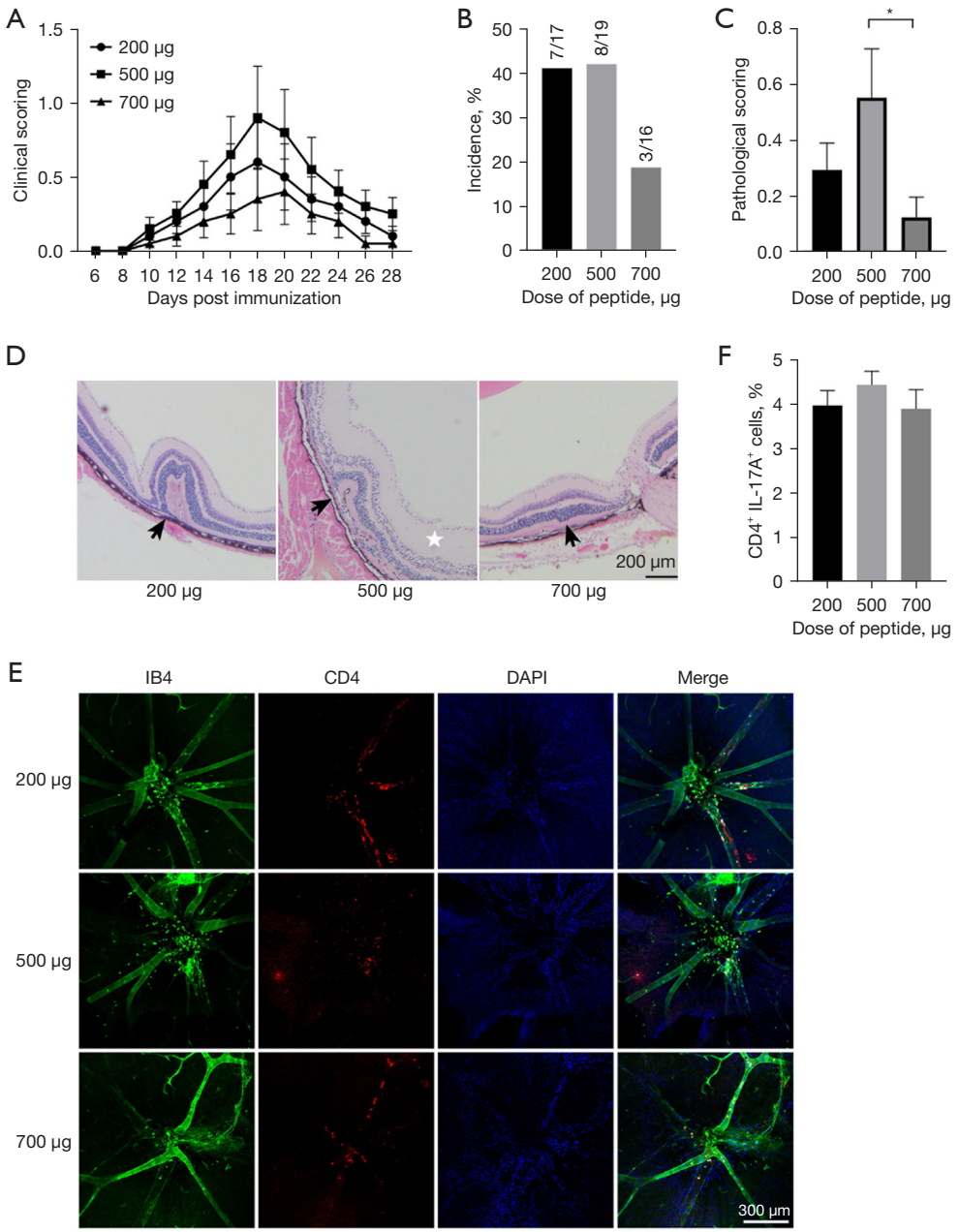

Figure 2 Influence of $IRBP_{1-20}$ dosage on EAU induction. EAU was induced in C57BL/6 mice (female, 6–8 weeks) by immunization with different dosages of $IRBP_{1-20}$ emulsified in CFA, with an intraperitoneal injection of 500 ng PTX simultaneously. (A) Clinical score at indicated time points postimmunization (n≥10). (B) Incidence of EAU in different dosage group: 200 μg (n=17), 500 μg (n=19), and 700 μg (n=16). Mice were sacrificed 18 days postimmunization. The number presents EAU mice/total immunized mice. (C) Mean pathological scores of HE retinal sections; *, P<0.05. The overall pathological scores include mice with EAU and mice without EAU (score 0). (D) Representative HE staining images of EAU in different dosage groups (black arrow: retinal folds; white star: edema; scale bar: 200 μm). (E) Representative immunofluorescent staining images for retina flat mounts (IB4: green, $CD4^+$ cells: red, DAPI: blue, scale bar: 300 μm). (F) Ratios of $CD4^+IL\text{-}17A^+$ cells in dLN, gated on $CD4^+$ cells (n=5). All data are presented as mean ± SEM. IB4, isolectin-B4; DAPI, 4,6-diamidino-2-phenylindole; IRBP, interphotoreceptor retinoid-binding protein; EAU, experimental autoimmune uveitis; CFA, complete Freund's adjuvant; PTX, pertussis; HE, hematoxylin and eosin; IL-17, interleukin-17; dLN, draining lymph node; SEM, standard error of the mean.

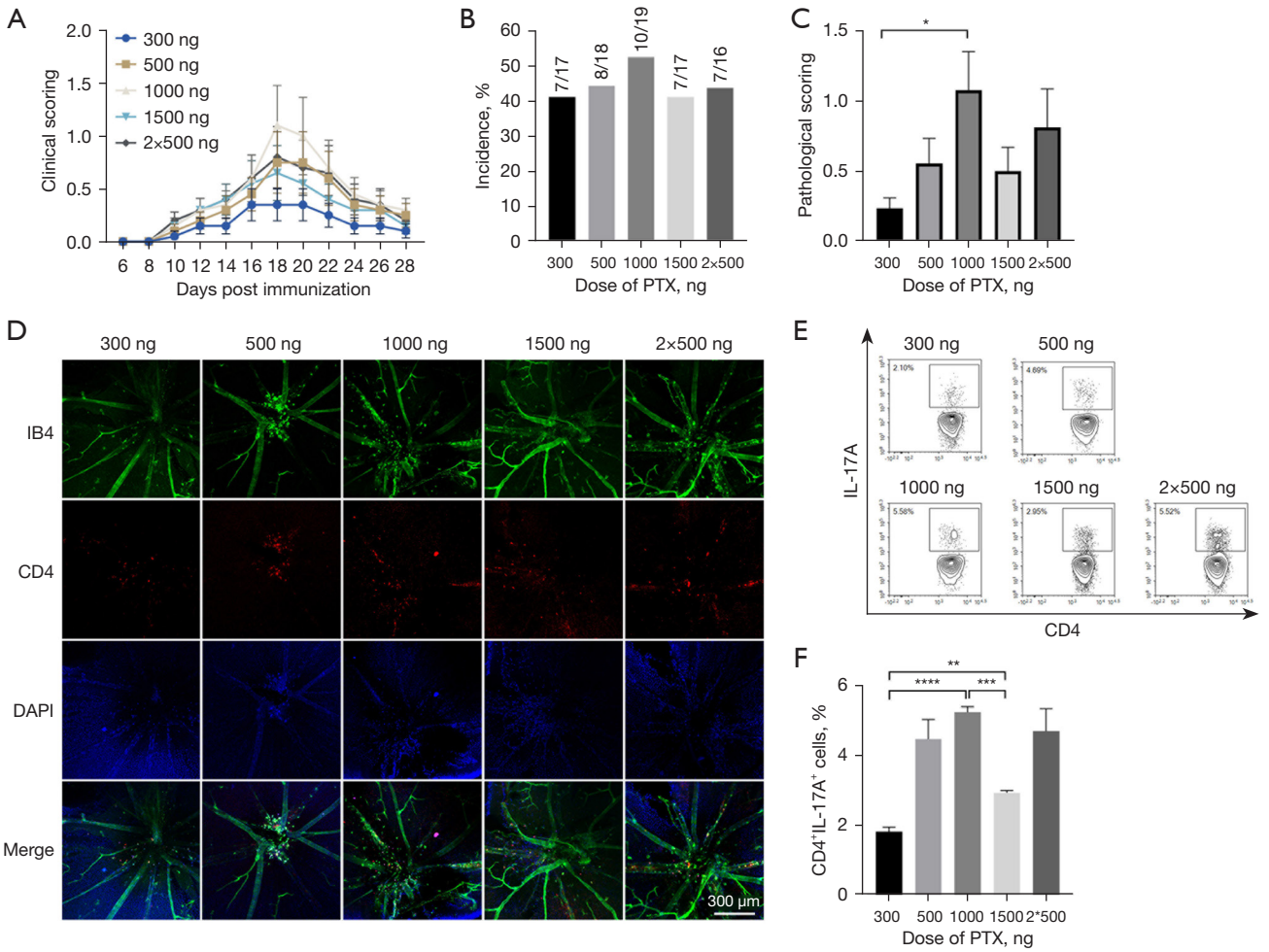

Figure 3 Influence of PTX dosage on EAU induction. EAU was induced in C57BL/6 mice (female, 6–8 weeks) by immunization with 500 μg of $IRBP_{1-20}$ emulsified in CFA, with an intraperitoneal injection of different dosages of PTX simultaneously. (A) Clinical score at indicated time points postimmunization (n≥10). (B) Incidence of EAU in groups: 300 ng (n=17), 500 ng (n=16), 1,000 ng (n=19), 1,500 ng (n=17), and 2×500 ng (splitting administration of 1,000 ng PTX into 2 dosages of 500 ng PTX on day 0 and day 2; n=16). Mice were sacrificed 18 days postimmunization. The number presents EAU mice/total immunized mice. (C) Mean pathological scores of HE retinal sections; *, P<0.05. The overall pathological scores include mice with EAU and mice without EAU (score 0). (D) Representative immunofluorescent staining images for retina flat mounts (IB4: green, $CD4^+$ cells: red, DAPI: blue. scale bar: 300 μm). (E,F) Representative images of flowcytometry and ratios of $CD4^+IL\text{-}17A^+$ cells in dLN, gated on $CD4^+$ cells (n=5); **, P<0.01, ***, P<0.001, ****, P<0.0001. All data are presented as mean ± SEM. PTX, pertussis; IB4, isolectin-B4; DAPI, 4,6-diamidino-2-phenylindole; IL-17, interleukin-17; EAU, experimental autoimmune uveitis; IRBP, interphotoreceptor retinoid-binding protein; CFA, complete Freund's adjuvant; HE, hematoxylin and eosin; dLN, draining lymph node; SEM, standard error of the mean.

dLN showed no significant difference among the 3 groups (*Figure 2F*). Hence, the dosage of 500 μg was selected as the optimal dosage for subsequent experiments.

The optimal dosage of PTX

According to previous studies (11,18,20,24), 4 PTX doses (300, 500, 1,000, 1,500 ng) and 2 injection protocols (a single injection of 1,000 ng on day 0 and 2 injections of 500 ng PTX on day 0 and day 2) were adopted to assess the incidence and severity of EAU. The 1,000 ng PTX group exhibited the highest clinical score (*Figure 3A*). The histological results showed a similar EAU incidence (around 42%) among the different PTX-dose groups (*Figure 3B*).

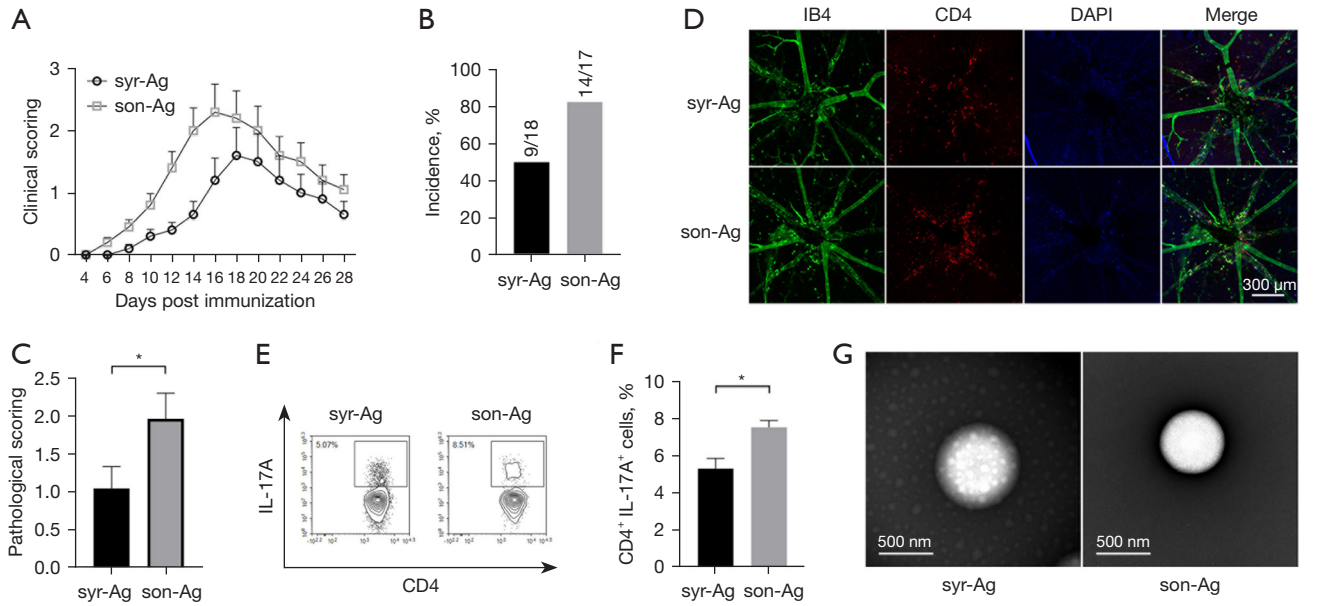

Figure 4 Different methods for emulsification in EAU induction. EAU was induced in C57BL/6 mice (female, 6–8 weeks) by immunization with 500 μg of $IRBP_{1-20}$ emulsified in CFA with an intraperitoneal injection of 1,000 ng of PTX simultaneously. Emulsions were performed with syr-Ag or son-Ag, respectively. Mice were sacrificed 18 days postimmunization. (A) Clinical score at indicated time points postimmunization (n≥10). (B) Incidence of EAU in different groups: syr-Ag (n=18) and son-Ag (n=17). The number represents EAU mice/total immunized mice. (C) Mean pathological scores of HE retinal sections; *, P<0.05. The overall pathological scores include mice with EAU and mice without EAU (score 0). (D) Representative immunofluorescent staining images for retina flat mounts (IB4: green, $CD4^+$ cells: red, DAPI: blue; scale bar: 300 μm). (E,F) Representative images of flow cytometry and ratios of $CD4^+IL\text{-}17A^+$ cells in dLN, gated on $CD4^+$ cells (n=5); *, P<0.05. (G) Representative images of the transmission electron microscope for each emulsion. All data are presented as mean ± SEM. EAU, experimental autoimmune uveitis; IRBP, interphotoreceptor retinoid-binding protein; CFA, complete Freund's adjuvant; PTX, pertussis; syr-Ag, syringe antigen/adjuvant extrusion; son-Ag, sonication antigen/adjuvant emulsion; HE staining, hematoxylin and eosin staining; IB4, isolectin-B4; DAPI, 4, 6-diamidino-2-phenylindole; dLN, draining lymph node; IL-17, interleukin 17; SEM, standard error of the mean.

For the histological scores, the 1,000 ng group showed the highest score (about 1.1), while the 500 and 1,500 ng groups showed moderate scores (around 0.5) and the 300 ng group showed the lowest score (about 0.2; *Figure 3C*). Consistent with the histological results, the most significant infiltration of $CD4^+$ T in the retina was observed in the 1,000 ng group (*Figure 3D*). The proportions of the Th17 population in the 500 and 1,000 ng groups were higher than those in the other 2 groups (*Figure 3E,3F*). In addition, the clinical and pathological scores and Th17 percentages showed no significant differences between the single injection with 1,000 ng of PTX and 2 injections with 500 ng of PTX (*Figure 3*). Therefore, a single injection of 1,000 ng PTX was applied for the subsequent experiments.

The methods of emulsification

The effective emulsification of adjuvant and antigen is essential to induce a sufficient autoimmune response (28,29). Given the low EAU incidence in the C57BL/6 strain, 2 different emulsification approaches were tested for EAU induction: the traditional emulsification extruded with 2 interconnected syringes (syr-Ag) and the sonicated antigen/adjuvant emulsification (son-Ag). Interestingly, the son-Ag group exhibited higher clinical scores of EAU than did the sry-Ag group (*Figure 4A*). The EAU peak of the son-Ag group appeared at 16–18 days after immunization, approximately 2 days earlier than that of the syr-Ag group (*Figure 4A*). Moreover, the son-Ag group also showed a higher EAU incidence (about 82%) and higher pathological

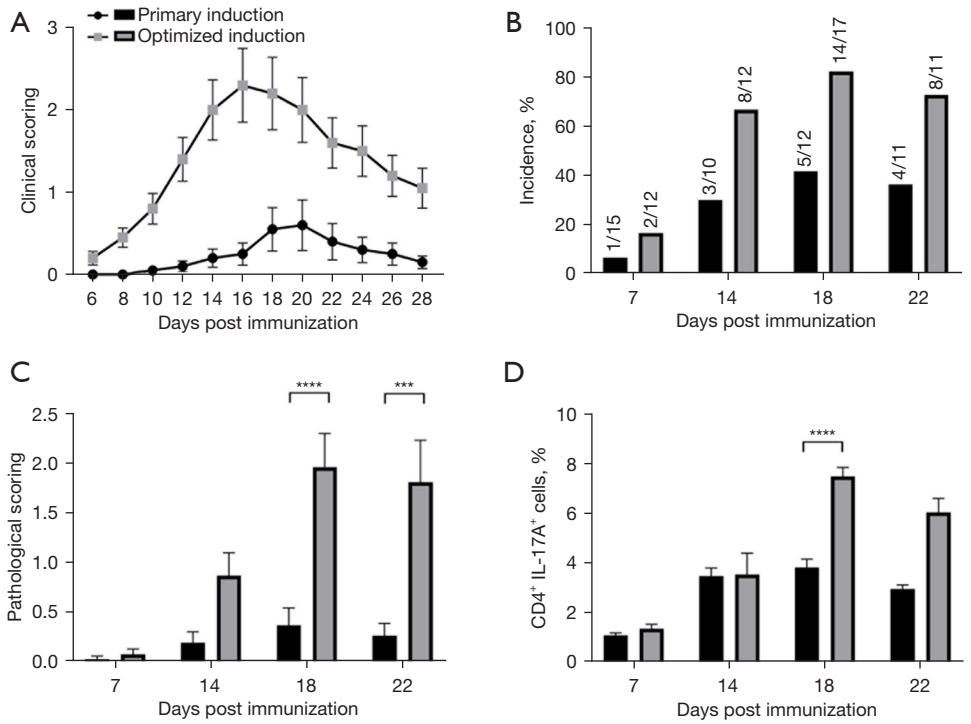

Figure 5 Head-to-head comparison between primary and optimized induction. EAU was induced in C57BL/6 mice (female, 6–8 weeks) by immunization with a primary and optimized protocol, respectively. (A) Clinical score at indicated time points postimmunization with different induction protocols (n≥10). (B) Incidence of EAU in different groups at indicated time points. The number presents EAU mice/total immunized mice. (C) Mean pathological scores of HE retinal sections at indicated time points; ***, P<0.001, ****, P<0.0001. The overall pathological scores include mice with EAU and mice without EAU (score 0). (D) Ratios of $CD4^+IL\text{-}17A^+$ cells in dLN, gated on $CD4^+$ cells at indicated time points (n=5); ****, P<0.0001. All data are presented as mean ± SEM. EAU, experimental autoimmune uveitis; HE staining, hematoxylin and eosin staining; dLN, draining lymph node; IL-17, interleukin 17; SEM, standard error of the mean.

score (around 2.0; P<0.05; *Figure 4B,4C*). The retinal flat mounts also revealed more retinal infiltration of $CD4^+$ T cells in the son-Ag group than in the syr-Ag group (*Figure 4D*). A higher proportion of Th17 cells in the dLN was detected in the son-Ag group (P<0.05; *Figure 4E,4F*). Importantly, electronic microscopy revealed that the vesicles of emulsion in the son-Ag group were significantly smaller than those in the syr-Ag group. This might have contributed to the different efficiency of EAU induction (*Figure 4G*).

Head-to-head comparison between the primary and optimized protocols for EAU induction

The efficiencies of EAU induction between the primary protocol (200 μg IRBP and 500 μg PTX, extruded emulsion; *Figure 1*) and the optimized protocol (500 μg IRBP and 1,000 μg PTX, sonicated emulsion; *Figure 4*) were compared. The optimized protocol group showed more severe inflammation and an earlier peak of EAU (days 16–18) than did the primary protocol group (days 18–20; *Figure 5A*). Moreover, higher incidence (82.4% *vs.* 37.5%) and pathological scores (2.0 *vs.* 0.3) were observed in the optimized protocol group on day 18 (*Figure 5B,5C*). The percentages of Th17 cells in the dLN were significantly elevated (7.53% for optimized protocol *vs.* 5.31% for primary protocol; *Figure 5D*). Therefore, the efficacy of EAU induction using our optimized protocol was higher than that using the primary protocol to some extent.

Discussion

The successful establishment of the EAU model is essential for the research of uveitis. However, the unstable EAU incidence in C57BL/6 mice leads to high experimental costs, confusion of experimental results, and extra

consumption of experimental animals. In previous studies, the EAU induction rates in C57BL/6 mice have varied in the ranges of 30–70%, and pathological scores have been mostly around 0.5–2 (10,11,20,23,24,30). The large variation of EAU induction among laboratories may be ascribed to multiple influencing factors, including dosage of reagents, degree of emulsification, and age of experimental animals. Optimizing the relevant conditions to obtain stable and sufficient EAU induction will be of great importance for EAU studies using C57BL/6 mice.

Currently, different types of peptide are available for EAU induction in rats or mice. Retinal soluble antigen (S-Ag) is commonly used in rats, while IRBP is mostly used in mice, with different mice strains manifesting different susceptibilities (26,31). Of note, the optimal dosage of $IRBP_{1-20}$ is central to the induction rate. Too high a dosage may cause T cell apoptosis or may induce T regulatory cells instead and, hence, suppress the immune response (32,33). Our data suggested that only the appropriate peptide dose was useful for enhancing induction efficacy and inflammation severity, and 500 μg $IRBP_{1-20}$ might be the optimal dosage for EAU induction in C57BL/6 mice (*Figure 2*).

PTX can open the blood–retina barrier and enhance the Th1 and Th17 response in EAU (11,18,20,24). Administration of PTX permits the occurrence of EAU in resistant strains and enhancement of EAU inflammation in susceptible strains (6). In the Lewis rat EAU model, PTX is not indispensable for the immunization protocol to develop EAU and, if used, can cause an earlier onset and enhanced disease scores (15). However, PTX can also inhibit the chemokine receptor signaling pathways promoting cell migration to target organs and lead to inhibitory effects on diseases (34). In an experimental autoimmune encephalomyelitis (EAE) study, the administration of PTX was split into 2 injections (35). In our study, the dosage of PTX made no difference to the EAU induction rate but could influence the intensity of the immune response. Although no statistically significant differences in histological scores or the proportion of Th17 cells were observed between the 1,000 and 500 ng PTX doses, 1,000 ng PTX seemed to induce a more severe immune response and EAU lesions (*Figure 3*). Our data highlighted the importance of PTX dosage in the severity of induced EAU. A single injection of 1,000 ng might be the optimal configuration in C57BL/6 mice.

The emulsification technique has been adopted in various autoimmune disease models. In EAE, the emulsification methods were found to play a role in the induction of inflammation (26,28). The sonicated antigen/adjuvant emulsion was shown to effectively induce EAE in the DBA/2 (H-2d) strain, whereas the conventional extruded emulsion only produced resistant EAE (29). In our work, the sonicated emulsion method had a better effect on EAU induction, with a higher EAU incidence of 82.4% and an earlier inflammation peak (*Figure 4*). The smaller vesicle diameter in the sonicated emulsion group, as shown in electron microscopy (*Figure 4G*), may facilitate accessibility for antigen-presenting cells and, hence, antigen presentation.

Our study adopted several approaches to assessing EAU, including fundus observation, HE staining, and retinal whole flat mounts. Fundus observation provided direct, continuous, and fundamental information on EAU lesions. HE staining is regarded as the gold standard for histopathological assessment in EAU (15,36-38). The consensus is that the infiltration of inflammatory cells and structural changes are more likely to occur near the optic nerve disc (8). However, discrepancy in the scoring results for different sections of a single eye was observed in our laboratory. This may be ascribed to the missing of some part of the inflammatory zone in the single HE section. Compared with the above two approaches, the retinal whole flat mounts allowed a more comprehensive assessment of inflammatory infiltration and local lesion changes (39-41). However, a limitation was the absence of scoring criteria to quantitatively assess the intensity of inflammation (39-41). Therefore, the strategy of involving multiple approaches in the assessment of EAU should be considered reasonable for obtaining more reliable scoring results, as each approach has its merits and weaknesses.

In conclusion, this work attempted to optimize the conditions of relevant factors which are crucial for the sufficient establishment of EAU in C57BL/6 mice. With the conditions of 200 μg of $IRBP_{1-20}$, 500 ng of PTX, and extruded emulsification, the induction rate was only 37.5% and the pathological score was around 0.3, whereas with the optimized induction conditions (500 μg $IRBP_{1-20}$, 1,000 ng PTX, and ultrasound emulsification), the induction rate was increased to 82.4% and the pathological score was around 2.0 (*Figure 5B,5C*). The protocol with 500 μg of peptide, 1,000 ng of PTX, and sonicated emulsion seemed to be optimal for stable and high induction rate of EAU with sufficient inflammation severity in the C57BL/6 mice strain, as evidenced by the multiple assessment approaches.

Acknowledgments

We would like to thank the Key Laboratory of Immunity and Inflammatory Diseases of Zhejiang Province for the experimental platform of uveitis.

Funding: This work was supported by the National Natural Science Foundation of China (No. 81670842).

Footnote

Reporting Checklist: The authors have completed the ARRIVE reporting checklist. Available at https://atm.amegroups.com/article/view/10.21037/atm-22-2293/rc

Data Sharing Statement: Available at https://atm.amegroups.com/article/view/10.21037/atm-22-2293/dss

Peer Review File: Available at https://atm.amegroups.com/article/view/10.21037/atm-22-2293/prf

Conflicts of Interest: All authors have completed the ICMJE uniform disclosure form (available at https://atm.amegroups.com/article/view/10.21037/atm-22-2293/coif). The authors have no conflicts of interest to declare.

Ethical Statement: The authors are accountable for all aspects of the work in ensuring that questions related to the accuracy or integrity of any part of the work are appropriately investigated and resolved. All animal experiments were approved by the tab of animal experimental ethical inspection of the First Affiliated Hospital, College of Medicine, Zhejiang University (Ethical Approval No. 2019-23-1) and were carried out in accordance with the Guide for the Care and Use of Laboratory Animals, 8th edition.

References

1. Tsirouki T, Dastiridou A, Symeonidis C, et al. A Focus on the Epidemiology of Uveitis. Ocul Immunol Inflamm 2018;26:2-16.
2. Selmi C. Diagnosis and classification of autoimmune uveitis. Autoimmun Rev 2014;13:591-4.
3. Caspi RR. A look at autoimmunity and inflammation in the eye. J Clin Invest 2010;120:3073-83.
4. Gasparin F, Takahashi BS, Scolari MR, et al. Experimental models of autoimmune inflammatory ocular diseases. Arq Bras Oftalmol 2012;75:143-7.
5. Silver PB, Rizzo LV, Chan CC, et al. Identification of a major pathogenic epitope in the human IRBP molecule recognized by mice of the H-2r haplotype. Invest Ophthalmol Vis Sci 1995;36:946-54.
6. Silver PB, Chan CC, Wiggert B, et al. The requirement for pertussis to induce EAU is strain-dependent: B10.RIII, but not B10.A mice, develop EAU and Th1 responses to IRBP without pertussis treatment. Invest Ophthalmol Vis Sci 1999;40:2898-905.
7. Chen Y, Chen Z, Chong WP, et al. Comparative Analysis of the Interphotoreceptor Retinoid Binding ProteinInduced Models of Experimental Autoimmune Uveitis in B10.RIII versus C57BL/6 Mice. Curr Mol Med 2018;18:602-11.
8. Xu H, Koch P, Chen M, et al. A clinical grading system for retinal inflammation in the chronic model of experimental autoimmune uveoretinitis using digital fundus images. Exp Eye Res 2008;87:319-26.
9. Klimova A, Seidler Stangova P, Svozilkova P, et al. The critical points in induction of experimental autoimmune uveitis. Biomed Pap Med Fac Univ Palacky Olomouc Czech Repub 2016;160:140-2.
10. Mattapallil MJ, Silver PB, Cortes LM, et al. Characterization of a New Epitope of IRBP That Induces Moderate to Severe Uveoretinitis in Mice With H-2b Haplotype. Invest Ophthalmol Vis Sci 2015;56:5439-49.
11. Fang J, Fang D, Silver PB, et al. The role of TLR2, TRL3, TRL4, and TRL9 signaling in the pathogenesis of autoimmune disease in a retinal autoimmunity model. Invest Ophthalmol Vis Sci 2010;51:3092-9.
12. Yadav UC, Shoeb M, Srivastava SK, et al. Aldose reductase deficiency protects from autoimmune- and endotoxin-induced uveitis in mice. Invest Ophthalmol Vis Sci 2011;52:8076-85.
13. Yazid S, Gardner PJ, Carvalho L, et al. Annexin-A1 restricts Th17 cells and attenuates the severity of autoimmune disease. J Autoimmun 2015;58:1-11.
14. Klaska IP, Muckersie E, Martin-Granados C, et al. Lipopolysaccharide-primed heterotolerant dendritic

cells suppress experimental autoimmune uveoretinitis by multiple mechanisms. Immunology 2017;150:364-77.
15. Agarwal RK, Silver PB, Caspi RR. Rodent models of experimental autoimmune uveitis. Methods Mol Biol 2012;900:443-69.
16. Shao H, Liao T, Ke Y, et al. Severe chronic experimental autoimmune uveitis (EAU) of the C57BL/6 mouse induced by adoptive transfer of IRBP1-20-specific T cells. Exp Eye Res 2006;82:323-31.
17. Zhang Y, Li Y, Liu P, et al. Phosphatase Shp2 regulates biogenesis of small extracellular vesicles by dephosphorylating Syntenin. J Extracell Vesicles 2021;10:e12078.
18. Avichezer D, Silver PB, Chan CC, et al. Identification of a new epitope of human IRBP that induces autoimmune uveoretinitis in mice of the H-2b haplotype. Invest Ophthalmol Vis Sci 2000;41:127-31.
19. Fukushima A, Yamaguchi T, Ishida W, et al. Mice lacking the IFN-gamma receptor or fyn develop severe experimental autoimmune uveoretinitis characterized by different immune responses. Immunogenetics 2005;57:337-43.
20. Santeford A, Wiley LA, Park S, et al. Impaired autophagy in macrophages promotes inflammatory eye disease. Autophagy 2016;12:1876-85.
21. Ke Y, Sun D, Zhang P, et al. Suppression of established experimental autoimmune uveitis by anti-LFA-1alpha Ab. Invest Ophthalmol Vis Sci 2007;48:2667-75.
22. Hsu SM, Yang CH, Tsai HY, et al. Chitosan Oligosaccharides Suppress Nuclear Factor-Kappa B Activation and Ameliorate Experimental Autoimmune Uveoretinitis in Mice. Int J Mol Sci 2020;21:8326.
23. Cortes LM, Mattapallil MJ, Silver PB, et al. Repertoire analysis and new pathogenic epitopes of IRBP in C57BL/6 (H-2b) and B10.RIII (H-2r) mice. Invest Ophthalmol Vis Sci 2008;49:1946-56.
24. Pan S, Tan H, Chang R, et al. High Ambient Temperature Aggravates Experimental Autoimmune Uveitis Symptoms. Front Cell Dev Biol 2021;9:629306.
25. Huang Y, He J, Liang H, et al. Aryl Hydrocarbon Receptor Regulates Apoptosis and Inflammation in a Murine Model of Experimental Autoimmune Uveitis. Front Immunol 2018;9:1713.
26. Chen N, Chen S, Zhang Z, et al. Overexpressing Kallistatin Aggravates Experimental Autoimmune Uveitis Through Promoting Th17 Differentiation. Front Immunol 2021;12:756423.
27. Li X, Gao Q, Yang L, et al. Matairesinol ameliorates experimental autoimmune uveitis by suppression of IRBP-specific Th17 cells. J Neuroimmunol 2020;345:577286.
28. Määttä JA, Erälinna JP, Röyttä M, et al. Physical state of the neuroantigen in adjuvant emulsions determines encephalitogenic status in the BALB/c mouse. J Immunol Methods 1996;190:133-41.
29. Määttä JA, Nygårdas PT, Hinkkanen AE. Enhancement of experimental autoimmune encephalomyelitis severity by ultrasound emulsification of antigen/adjuvant in distinct strains of mice. Scand J Immunol 2000;51:87-90.
30. Fu Q, Man X, Wang X, et al. CD83+ CCR7+ NK cells induced by interleukin 18 by dendritic cells promote experimental autoimmune uveitis. J Cell Mol Med 2019;23:1827-39.
31. Haruta H, Ohguro N, Fujimoto M, et al. Blockade of interleukin-6 signaling suppresses not only th17 but also interphotoreceptor retinoid binding protein-specific Th1 by promoting regulatory T cells in experimental autoimmune uveoretinitis. Invest Ophthalmol Vis Sci 2011;52:3264-71.
32. Liblau RS, Tisch R, Shokat K, et al. Intravenous injection of soluble antigen induces thymic and peripheral T-cells apoptosis. Proc Natl Acad Sci U S A 1996;93:3031-6.
33. Xu H, Feldman GM, Max EE. High-Dose IV Administration of Rasburicase Suppresses Anti-rasburicase Antibodies, Depletes Rasburicase-Specific Lymphocytes, and Upregulates Treg Cells. AAPS J 2020;22:80.
34. Su SB, Silver PB, Zhang M, et al. Pertussis toxin inhibits induction of tissue-specific autoimmune disease by disrupting G protein-coupled signals. J Immunol 2001;167:250-6.
35. Ahn BJ, Le H, Shin MW, et al. Ninjurin1 deficiency attenuates susceptibility of experimental autoimmune encephalomyelitis in mice. J Biol Chem 2014;289:3328-38.
36. Chen Y, Li Z, Li H, et al. Apremilast Regulates the Teff/Treg Balance to Ameliorate Uveitis via PI3K/AKT/FoxO1 Signaling Pathway. Front Immunol 2020;11:581673.
37. Ko MK, Shao H, Kaplan HJ, et al. Timing Effect of Adenosine-Directed Immunomodulation on Mouse Experimental Autoimmune Uveitis. J Immunol 2021;207:153-61.
38. Li H, Zhu L, Wang R, et al. Therapeutic Effect of IL-38 on Experimental Autoimmune Uveitis: Reprogrammed Immune Cell Landscape and Reduced Th17 Cell Pathogenicity. Invest Ophthalmol Vis Sci 2021;62:31.
39. Chu CJ, Herrmann P, Carvalho LS, et al. Assessment and in vivo scoring of murine experimental autoimmune

uveoretinitis using optical coherence tomography. PLoS One 2013;8:e63002.
40. Dick AD, Forrester JV, Liversidge J, et al. The role of tumour necrosis factor (TNF-alpha) in experimental autoimmune uveoretinitis (EAU). Prog Retin Eye Res 2004;23:617-37.
41. Umazume A, Kezuka T, Matsuda R, et al. Role of PU.1 Expression as an Inflammatory Marker in Experimental Autoimmune Uveoretinitis. Ocul Immunol Inflamm 2018;26:951-63.

(English Language Editors: K. Gilbert and J. Gray)

Cite this article as: Yang M, Yang Z, Huang J, Yu W, He X, Yuan M, Han W, Chen W. Optimization of determinant factors associated with the efficiency of experimental autoimmune uveitis induction in C57BL/6 mice. Ann Transl Med 2022;10(23):1274. doi: 10.21037/atm-22-2293